SAND2006-4393C

Damage Equivalence of Heavy Ions in Silicon Bipolar Junction Transistors

E. Bielejec, G. Vizkelethy, N. R. Kolb, D. B. King, and B. L. Doyle

Abstract— Results of displacement damage correlation between neutrons, light ions and heavy ions in bipolar junction transistors will be presented. Gain degradation as the function of fluence was measured. The gain degradation due to heavy ion irradiation followed the Messenger-Spratt equation, while some deviation was found for light ions.

***Index Terms*— damage equivalence, silicon bipolar transistor**

I. INTRODUCTION

Damage equivalence between different kinds of particles has been studied for some time. A recent excellent review is given in [1]. Using various light ions and neutrons on silicon bipolar junction transistors, Summers et al [2] showed that the damage ratio calculated from the Messenger-Spratt equation [3] scales with the Non-ionizing Energy Loss (NIEL). Recently, there is a new demand to determine ion-to-neutron damage equivalency since pulsed nuclear reactors producing high flux short neutron pulses are becoming less and less accessible. An alternative to pulsed neutron beams is to use a pulsed ion beam that produces the same displacement damage. The first step in this process is to establish the damage equivalency at late times. Most of the damage equivalency studies were done with light ions (protons to alphas) and there is very little data available for heavy ions. Warner *et al* [4] reported results for damage equivalency between 2 MeV protons and 22 MeV silicon ions in p+n GaAs solar cells. They concluded that the normalized photocurrent scaled with the displacement damage dose calculated from the NIEL for both ions. If the same damage equivalency can be established between heavy ions and neutrons, the neutron damage experiments can be simulated in a much simpler and safer environment. In this paper we report the first results of our damage equivalency study on 2n2222 bipolar junction transistors (BJT). We used the Sandia National Laboratories (SNL) nuclear microprobe facility to irradiate the BJTs with short, high flux ion pulses and measured the gain degradation as the function of accumulated fluence. We compared the results to similar measurements carried out with ultra short high neutron flux pulses at the Los Alamos Neutron Science Center (LANSCE). The results were compared to calculations based on SRIM-2003.

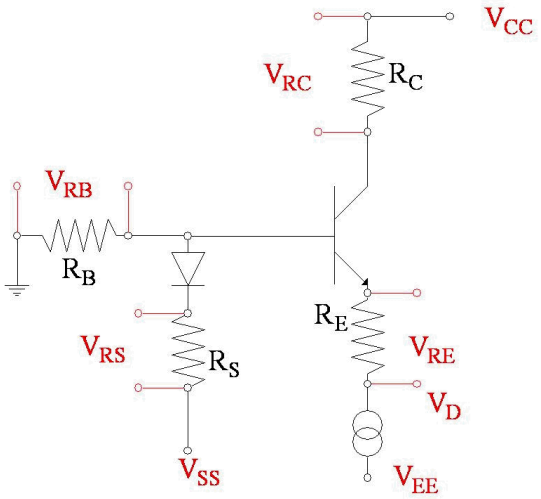

Fig. 1. The experimental circuit used in the ion beam measurements. This circuit was designed to minimize the effect of the ion induced photocurrent. The red lettering indicates the measurement points on the circuit.

II. EXPERIMENTAL DETAILS

Single diffusion lot 2n2222 bipolar junction transistors from Microsemi were used in these experiments. The ion irradiations were performed at the SNL nuclear microprobe facility. The ion beam was focused to a size somewhat larger than the size of the transistor die (~0.5x0.5 mm^2). The ion beam was pulsed using electrostatic deflection plates and a high voltage switch

Manuscript received July 14, 2006. Sandia is a multiprogram laboratory operated by Sandia Corporation, a Lockheed-Martin Company, for the United States Department of Energy's National Nuclear Security Administration under contract DE-AC04-94AL85000.

E. Bielejec is with Sandia National Laboratories, Albuquerque, NM 87185 USA (505-284-9256; fax: 505-844-7775; e-mail: esbiele@sandia.gov).

G. Vizkelethy is with Sandia National Laboratories, Albuquerque, NM 87185 USA (e-mail: gvizkel@sandia.gov).

N. R. Kolb is with Science Applications International Corporation, Albuquerque, NM 87106 USA (e-mail: nkolb@sandia.gov).

D. B. King is with Sandia National Laboratories, Albuquerque, NM 87185 USA (e-mail: dbking@sandia.gov).

D. L. Doyle is with Sandia National Laboratories, Albuquerque, NM 87185 USA (e-mail: dldoyle@sandia.gov).

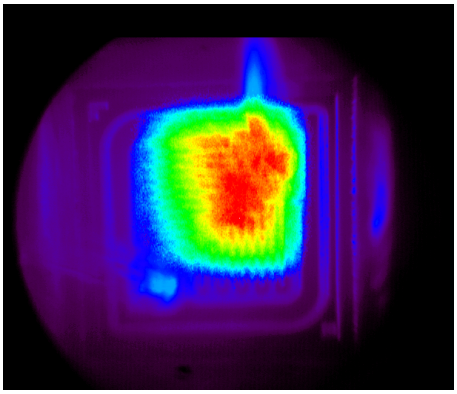

Fig. 2. Combined picture of the device and the incidence beam spot showing typical alignment as well as the profile of the beam. The color scale green to red indicates a 1/3 drop in signal. The structure apparent in the beam spot is due to an artifact of the convolution of the two pictures and does not appear in the beam spot alone.

with rise and fall times of 150 ns. The neutron irradiations were performed at LANSCE with a maximum 1 MeV equivalent neutron fluence of 2.75×10^{13} n/cm^2. The LANSCE facility was used to supply short pulses of protons or neutrons. The LINAC section generates proton ions of energies ranging from 250 – 800 MeV with a micropulse width of 0.1 ns every 5 ns at multiples of 180 ns, resulting in $3\text{-}5 \times 10^8$ protons/micropulse. The proton beams are stored in the proton storage ring. The proton rate supplied to the target can range from a single shot mode up to a 20 Hz operation. Approximately 1×10^{12} to 4×10^{13} protons are supplied per pulse with a 260 ns full width at base, 150 ns FWHM. Spallation neutrons were produced from 800 MeV protons incident on a 2"x2"x6" target of tungsten. The irradiated devices are placed as close as possible to the surface of the target to maximize the neutron fluence per proton pulse. The test articles were exposed to approximately 2×10^{12} neutrons/cm^2 (1 MeV Si eq) and 1×10^3 rad(Si) per pulse. The irradiated devices were enclosed in a RF-shielded test head and cables run through flexible conduit to reduce noise pickup. The operation of the transistors was typically monitored for 10 ms after a single proton pulse.

In both the ion and neutron irradiations the currents of the transistor were monitored using current viewing resistors before, during, and after the shots. The voltages across the current viewing resistors were recorded with a Yokogawa DL750P oscilloscope-recorder. The circuit diagram of the experiment is shown in Fig. 1 with red lettering indicating the measurement points. The transistors were operated in constant emitter current mode, and the emitter current was provided by current limiting diodes. For the experiments described below the emitter current was either 0.22 mA or 7.7 mA. The purpose of the diode in the base leg circuit is to limit the photo current through the R_B resistor during the shot to avoid fast, large changes in the potential of the base electrode. In addition, a large resistor is used in the base leg to measure the base current accurately and to ensure that during the photocurrent response the base-current junction remains reverse biased. The gain of the transistor was determined from the collector and base currents before the shot and approximately 5 minutes

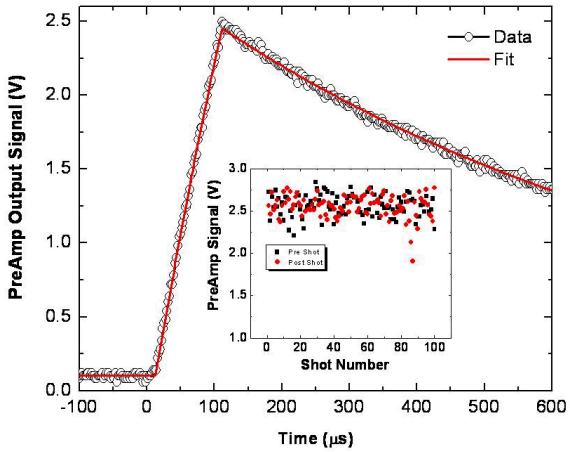

Fig. 3. The output of the Ortec 142A preamp as used as a charge integrator. Fitting the data determines the amplitude and duration of the signal. Inset: Shows a typical example of the comparison between one hundred shot into the preamp both before and after irradiation of the sample.

after the shot. This time interval seemed to be sufficient to consider the gain at this time as the late time gain with less than 5% error. The inverse gain degradation was then calculated according to the following equation:

$$D = \frac{1}{G} - \frac{1}{G_0} \qquad (1)$$

where G_0 and G are the initial gain and the final gain respectively. The inverse gain degradation will be compared for both neutron and ion irradiations.

Accurately knowing the incident fluence is of critical importance in these experiments. As a result, much time and effort was dedicated to determining and quantifying the uncertainty in the measured fluence. The fluence is determined by three components: beam area, pulse length and particle current.

To measure the beam area we captured a picture of the beam spot on a P47 phosphor film. This film has been chosen with the trade-off between adequate damage resistance and bright response to the incidence ions. By comparing the observed beam spot to a known scale, in our case a well defined TEM grid mounted on the sample holder, we are able to accurately determine the beam area. In addition, by using the phosphor film in an unsaturated state we are able to extract information regarding the beam profile and uniformity. As can be seen in Fig. 2, a combined picture of the device and the beam spot, we are limited to a beam spot of ~0.5x0.5 mm^2. This results in a beam profile that has a "hot" spot due to the profile of the beam. The experimental setup is being modified to allow for a larger spot size while maintaining the necessary current density, which will allow us to use only the center section of the beam spot, thus greatly improving our uniformity.

To measure the pulse length and particle current we use a cross-calibration method between a Keithley 6512 electrometer and either an Ortec 142A charge sensitive

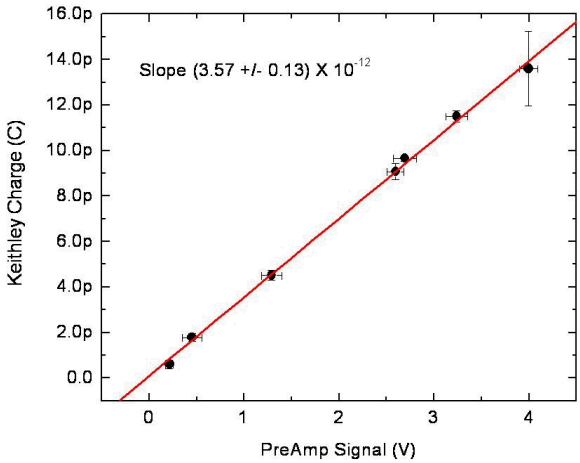

Fig. 4. Cross calibration of the preamp signal to the integrated charge during an ion pulse. This calibration is used to determine the particle current for each of the succeeding irradiation exposures.

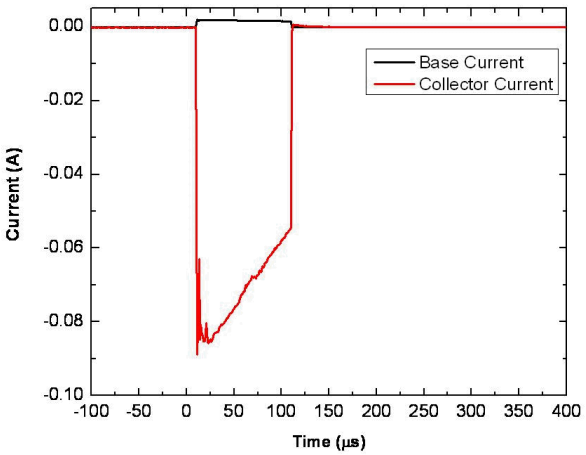

Fig. 5. Plot of the active transient measurement during a 28 MeV Si ion irradiation. The pulse length is nominally 100 μs with a measured fluence of 5.7×10^9 ions/cm^2.

preamplifier or a Keithley 428 current amplifier. The 142A is preferred for fast pulses with relatively low particle currents, while the 428 is used for pulses longer than 200 μs. A typical signal from the 142A is shown in Fig. 3. A series of shots at different pulse widths were taken and cross calibrated to the 6512. A calibration between the output signal of the 142A/428 and the charge collected, shown in Fig. 4, is the result. This calibration is then used to convert the succeeding amplifier signals into an integrated charge per pulse which determined the measured particle current of each irradiation exposure. This method provides an accurate measurement of the pulse length and particle current as well as information on time variations of the ion current during the pulse.

We have developed the techniques of imaging the beam spot and cross-calibration of the amplifiers to accurately determine the fluence on our samples. In practice, however, we are limited to a beam spot of only 0.5x0.5 mm^2; as a result this method cannot be *in-situ* with the irradiation. To address this we have automated the system such that we take and analyze 100 shots directly prior to irradiating the device and 100 shots directly after irradiation. The total time between measurements and irradiation of the device can be as short as 1 s. The variation between these before and after shots is used to bound the expected variation of the device irradiation (inset Fig. 3). By performing multiple exposures on different devices we are able to address both device-to-device as well as shot-to-shot variation.

In this experiment we used 3.9 MeV protons, 10 MeV, 28 MeV, 48 MeV Si ions, 12 MeV He, and 70 MeV I ions. We chose the 3.9 MeV protons because Summers reported results for this particular energy in [2]. The collector was kept at 10 V while the emitter current either 0.22 or 7.7 mA. The 0.22 mA case corresponds to an emitter-base voltage of ~0.6 V (medium injection) while 7.7 mA is ~0.7 V (high injection). The pulse lengths varied from 1 μs to 200 ms for the different ion beams. The maximum fluence for the 7.7 mA devices with an inverse gain degradation of 0.02 was the following: 3.9 MeV protons 2×10^{12}, 28 MeV Si 2×10^9, and 70 MeV I 3×10^7 ions/cm^2 respectively. For the 0.22 mA devices the inverse gain degradation was 0.2 and the maximum fluence was correspondingly much higher: 12 MeV He 1×10^{14}, 10 MeV Si 4×10^8, 28 MeV Si 7×10^9, and 48 MeV Si 2×10^{10} ions/cm^2.

III. RESULTS AND DISCUSSION

In Fig. 5 we plot the active transient response of the 2n2222 during irradiation with a 28 MeV Si ion beam. For the data shown the pulse length was 100 μs with a measured fluence of 5.7×10^9 ions/cm^2. During the pulse we observe a uniform decrease in the photocurrent response in both the collector and base leads due to damage in the device. Furthermore, we observe a large voltage response in both the measured diode voltage and the calculated emitter-base voltage during the pulse itself. The emitter voltage (monitoring the emitter current) is constant, as expected, with the exception of immediately at the start of and at the end of the pulse. This is due to the large photocurrent response during the pulse. Using the sum of the emitter, base, collector and shunt currents equaling zero as a test of the validation of the measurement we find that we can measure the device immediately after the pulse.

In general the NIEL approach is useful for light ions where the ions lose very little energy in the sensitive part of the device. In case of heavy ions, even at several tens of MeV energy, the energy of the ion significantly changes on a scale of few microns and this limits the use of the NIEL concept as it was pointed out in ref [5]. The paper's conclusion was that due to several factors (such as finite range, straggling, and energy carried away by recoils) the NIEL approach is valid if the changes in the NIEL are small in the sensitive region of the device. This means that the applicability of the NIEL approach depends not only on the particle and energy, but also on the device and on the parameter measured as the degree of damage. In BJTs the gain degradation occurs because of the

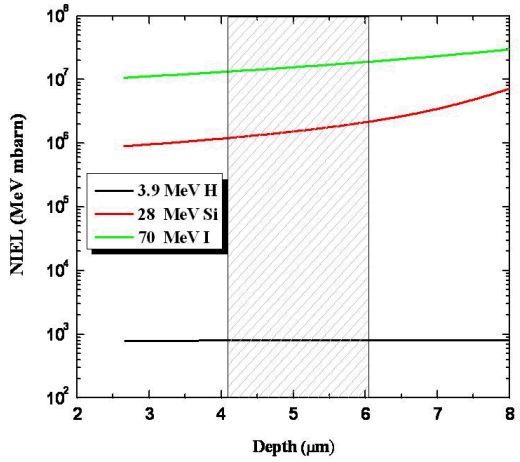

Fig. 6. Calculated NIEL as a function of depth in our 2n2222 device for several different ion beams.

increased recombination in the base region of the transistor. 1D model simulations [6] showed that the recombination occurs in a narrow region at the emitter base junction at low injection. Even at very high injection this region is confined within the base region which for this particular transistor is less than 2 μm. The energy loss by the proton beam in the full length of the transistor is negligible; therefore, we do not expect a problem for this ion beam. Fig. 6 shows the NIEL calculated using Robinson's formula [7]. The base area is shown as a hashed rectangle. Since we used 0.22 mA emitter current which corresponds to medium injection level we can calculate an average NIEL and compare it to the ones calculated for protons and neutrons.

From the inverse gain degradation as the function of fluence we calculate the damage factors for each particle using the Messenger-Spratt equation [3]:

$$D = k \cdot \Phi \qquad (2)$$

where Φ is the fluence, D is from equation (1), and k is a constant, the damage factor. Then we scaled these damage

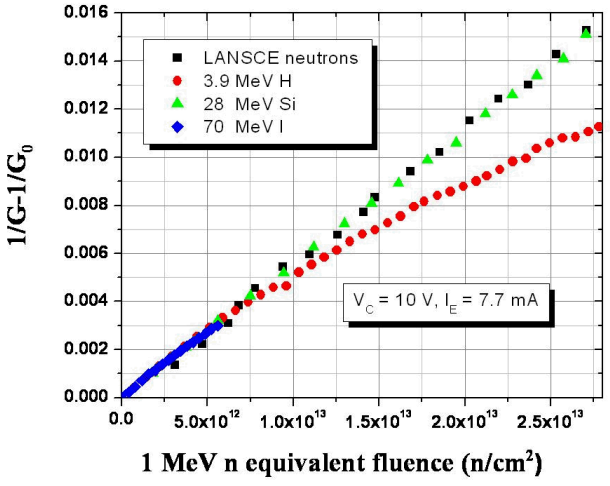

Fig. 7. Inverse gain degradation as a function of fluence for an emitter current of 7.7 mA.

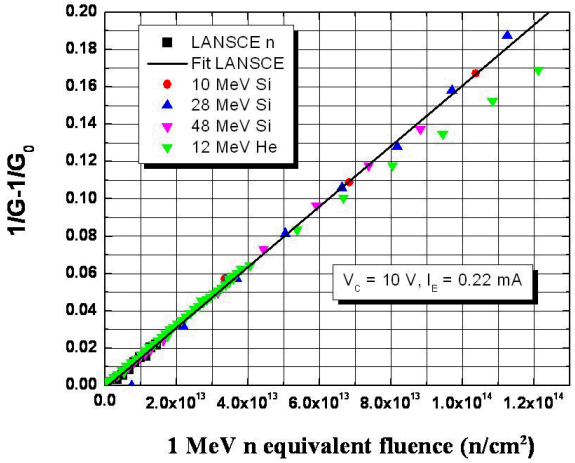

Fig. 8. . Inverse gain degradation as a function of fluence for an emitter current of 0.22 mA.

factors to the neutron damage factor and calculated the equivalent neutron fluence.

Fig. 7 and 8 show the inverse gain degradation as the function of the calculated equivalent neutron fluence. The heavy ion curves follow the predicted straight line, but the ones for protons and He deviate from the straight line at higher fluence. Similar behavior was shown in ref [8] in figure 1 for 2N2907 transistors under 4.1 MeV electron irradiation. At this point we assume that this non-linear behavior is caused by trapped charge in the passivation layer of the transistor. This effect is noticeable for the protons and He since the ionizing dose is significantly higher for the protons and He than for the heavy ions at the same gain degradation level. This assumption is supported by the Deep Level Spectroscopy (DLTS) measurements performed on the neutron, ion, and gamma irradiated transistors. While the DLTS spectrum was very similar for neutrons and heavy ions, for the protons, He and gamma irradiation a similar anomaly was observed in the DLTS spectrum [9].

TABLE 1

Current	Particle	Energy	K	k/k$_n$	NIEL	NIEL/NIEL$_n$
7.7 mA	LANSCE	spectrum	5.6x10^{-16}	1	95[10]	1
7.7 mA	proton	3.9 MeV	8.5x10^{-15}	15	1000	11
7.7 mA	Si	28 MeV	7.2x10^{-12}	13,000	2.1x10^{6}	22,000
7.7 mA	I	70 MeV	1.0x10^{-10}	190,000		
0.22 mA	LANSCE	spectrum	1.6x10^{-15}	1	95[10]	1
0.22 mA	He	12 MeV	3.0x10^{-13}	190	8000	84
0.22 mA	Si	10 MeV	5.2x10^{-10}	330,000	4.6x10^{7}	480,000
0.22 mA	Si	28 MeV	2.8x10^{-11}	18,000	2.1x10^{6}	22,000
0.22 mA	Si	48 MeV	1.3x10^{-11}	8,100	9.9x10^{5}	10,000

Table 1 shows the calculated damage factors, their ratio to the LANSCE neutron damage factors, the NIEL (in MeV mbarn) calculated using SRIM-2003 with 21 eV displacement

energy and the NIEL ratios to the 1 MeV neutron NIEL from reference [10] for both 7.7 and 0.22 mA emitter current data. The *k* factor for protons and He was calculated for the fluence where the inverse gain degradation seemed to be linear with the fluence. Our measured damage coefficient ratio for the 3.9 MeV protons differs slightly from the one measured by Summers [2] (11.3) but so does our calculated NIEL. The damage factors seem to scale with the calculated NIEL.

IV. Conclusion

We measured the inverse gain degradation of 2n2222 BJTs as the function of fluence using short pulsed light and heavy ion beams. The inverse gain degradation follows very well the Messenger-Spratt equation for heavy ions, but we found deviation from the linear behavior for light ions (proton/He) at higher fluence. We attribute this deviation to trapped charge in the passivation layer due to relatively higher ionization dose in case of the light ions. The comparison of the damage factors due to ion irradiation and the damage factor measured with LANSCE spallation neutrons showed that they are proportional to the theoretical NIEL values. Further studies of the damage equivalency of heavy ion irradiation are planned using a wider variety of ions, energies, and devices.

Acknowledgment

We acknowledge the outstanding support of D. Buller in running and maintaining the Sandia National Laboratories Nuclear Microprobe system.

References

[1] J. R. Sour, C. J. Marshall, and P. W. Marshall, "Review of displacement damage effects in silicon devices", IEEE Trans. Nucl. Sci. vol. 50, pp 653-670, 2003

[2] G. P. Summers, C. J. Dale, E. A. Burke, E. A. Wolicki, P. W. Marshall, and M. A. Gehlhausen, "Correlation of particle-induced displacement damage in silicon", *IEEE Trans. Nucl. Sci.* vol. 34, pp 1134-1139, 1987

[3] G. C. Messenger and J. P. Spratt, "The effects of neutron irradiation on silicon and germanium", *Proc. IRE* vol. 46, pp 1038-1044, 1958

[4] J. H. Warner, S. R. Messenger, R. J. Walters, and G. P. Summers, "Displacement damage correlation of proton and silicon irradiation in GaAs", *IEEE Trans Nucl. Sci.* vol. 52, pp 2678-2682, 2005

[5] S. R. Messenger, E. A. Burke, G. P. Summers, and R. J. Walters, "Limits to the application of NIEL for damage correlation", *IEEE Trans Nucl. Sci.* vol.51, pp3201-3206, 2004

[6] W. R. Wampler, private communications

[7] M. T. Robinson, "The energy dependence of neutron radiation damage in solids", Proc. of the British Nuclear Energy Society Conference on Nuclear Reactors, Culham, UK, September 17-19, 1969, pp 364-378

[8] C. J. Dale, P. W. Marshall, E. A. Burke, G. P. Summers, and E. A. Wolicki, "Hogh energy electron induced damage in silicon", *IEEE Trans Nucl. Sci.* vol.35, pp1208-121214, 1988

[9] R. M. Fleming, private communications

[10] ASTM Standard Methods E721-85 and ER2-85, Annual Book of ASTM Standards, ASTM, Philadelphia, Vol. 12.02, 1988.